A&A manuscript no.
(will be inserted by hand later)

Your thesaurus codes are:
12.03.2, 12.12.1

ASTRONOMY
AND
ASTROPHYSICS
5.2.2008

Pure Luminosity Evolution Hypothesis for QSOs: From Luminosity Functions to Synthetic Catalogues

G. Mathez[1], **L. Van Waerbeke**[1], **Y. Mellier**[1], **H. Bonnet**[1], **M. Lachièze-Rey**[2]

[1] Laboratoire d'Astrophysique de Toulouse, URA285. Observatoire Midi-Pyrénées 14, avenue Edouard Belin F-31400 - Toulouse
[2] CEN Saclay Service de Physique Théorique F-91191 Gif Cedex

Received ; accepted

Abstract. This paper describes the construction of realistic extragalactic Monte–Carlo catalogues, aimed at comparing the behaviour of cosmological tests versus input parameters. QSO catalogues are built on a luminosity function derived from data through a certain choice of any cosmological and evolutionary model, and through suitable computation of individual maximum volumes in complete (but magnitude– and redshift–limited) samples. Details of this computation are examined for the case of strong luminosity evolution. The values of the evolution parameter are derived for various cosmologies, corresponding to $< V/V_{max} >= 1/2$ in the sample of 400 Ultra–Violet Excess (UVX) QSOs (**?**). The various luminosity functions are compared, both for the whole sample and in redshift bins. A characteristic evolution time is defined and computed, depending strongly on the cosmology, but practically constant when expressed in terms of the age of the universe. Algorithms are given for producing catalogues based on the null hypothesis that the objects are uniformly distributed in volume but suffer pure luminosity evolution. The only input based on real data is the luminosity function, but this requires neither a redshift nor an apparent magnitude histogram. Simulated redshift and absolute magnitude histogrames are compared to real data.

Key words: Cosmology, Quasars, Numerical simulations

1. Introduction

Various judicious tests have been developed to discriminate between different cosmological models, all requiring large and complete samples of extragalactic objects (quasars or galaxies). Unfortunately, the available samples are magnitude limited, selection effects induce poorly known systematic biases in magnitude and redshift, and extragalactic populations undergo strong evolution over a Hubble time. This paper describes the construction of extragalactic synthetic catalogues with various parent cosmologies, evolution laws and simulated observational biases, with the goal of applying them to the cosmological test described in Paper I (**?**). A preliminary study of the luminosity function of the real population and of its evolution in various cosmologies is necessary for such a construction; so it is also a by product of the present paper.

The two main extragalactic populations, quasars and galaxies, may be simulated: we focus on quasars in the following since they are more distant and *a priori* more suited to cosmological tests. A quasar being by definition stellar in appearance, the pair of apparent magnitude–redshift (m, z) is sufficient to characterize it with respect to current cosmological tests. The result of the simulation is thus a list of apparent magnitudes and redshifts, *not* an image.

The observed population suffers strong evolution, as evinced by either the standard $< V/V_{max} >$ analyse or direct derivation of the luminosity function in redshift bins. Pure Luminosity Evolution (PLE) seems to be the best model (**?**), but Pure Density Evolution (PDE) or mixed models are not rejected; and the question remains open for redshifts greater than 2.2 (**?**). Paper I describes a cosmological test which accounts for such evolution.

Quasars also suffer various biases in their redshift distribution and a strong variability in luminosity. Our initial aim was to construct synthetic quasar catalogues capable of quantifying the behaviour of the test as a function of the various parameters:

- sensitivity to the cosmological parameters;
- photometric uncertainties and strong quasar variability;
- redshift uncertainties and biasing in certain redshift ranges;
- catalogue size and redshift limitations, leading to a preferred observational strategy for the construction of quasar samples;
- this list is certainly not exhaustive.

Last, but not least, most cosmological tests using QSOs rely on some basic assumption concerning their evolution. As a consequence, their result in principle applies only within this framework. With Monte–Carlo catalogues, it is possible to test the uncertainty induced by any false hypothesis on evolution by making cross–tests between different assumed evolutions: this may concern the nature of the evolution, either Density or Luminosity Evolution (DE/LE), as well as its functional form, PoWer law or EXPonential (PWLE/LEXP). The present paper addresses only the case of PLE. PDE will be the subject of a forthcoming paper.

The paper is organized as follows: in Section 2 the basic method is exposed. After a brief review of the cosmological

Send offprint requests to: G. Mathez

frame, the computation of volumes and maximum volumes is detailed in Section 3. In Section 4 the sample of Boyle is used to derive the necessary LF. In Section 5 the evolutionary parameters and characteristic times found in various cosmological models are compared. In Section 6 a general algorithm to construct artificial QSO samples is derived from our working hypotheses. The redshift and magnitude histogrames of synthetic catalogues are examined.

2. Basic Method

Previous numerical simulations have been performed in a similar way, essentially aimed at producing catalogues of galaxies. Chokshi *et al.* (**?**) simulate galaxies in clusters uniformly distributed in space. In each cluster, about 1,000 galaxies are drawn, all at the same redshift. The magnitudes are sorted according to the Schechter Luminosity Function (LF), brighter than a certain cut-off which of course depends on the cluster redshift. Yee (**?**) first sorts the apparent magnitude according to the observed distribution, the redshift is then computed in bins of apparent magnitude according to a certain Luminosity Function (LF) based on a given, fixed, cosmological and evolutionary model. Our method is slightly different: first, a functional form for the evolution is chosen, and the cosmological parameters are varied on a certain grid. There is then a unique evolution parameter ensuring the condition $< V/V_a >= 1/2$ for a given, actual, sample, V_a being the available comoving volume according to Avni *et al* (**?**). The zero–redshift LF Φ is fixed by such a procedure, and fitted according to some previous analytic choice for the LF. Once the evolution of the LF is known, $V_a(M_0)$ may be computed in terms of the zero–redshift absolute magnitude (M_0). The resulting probability distribution function *in the sample* of absolute magnitude is then $\Phi(M_0) \times V_a(M_0)$. It is easy to sort the absolute magnitude of object i according to this PDF. A second parameter, either the apparent magnitude or the redshift, is needed to define a QSO. Given the absolute magnitude M_0 and the cosmological and evolutionary model, $V_a(M_0)$ may be computed. A second random drawing according to a uniform distribution gives a number $x \in [0, 1]$, and the redshift of object i may be computed from the condition: $V = x \times V_a(M_0)$. (m, z), the apparent magnitude–redshift pair, is then derived from these two variables. For each cosmological model, the procedure is repeated until the desired catalogue size is reached.

The null hypotheses are: that PLE applies, that the luminosities are distributed according to the observed LF and that, according to the Cosmological Principle, the QSOs are uniformly distributed in volume on Gpc scales, so that the variable V/V_a is uniformly spread over $[0, 1]$. From the LF we are able to draw the two variables M_0, the zero–redshift absolute magnitude, and x; and from the assumption of uniformity we draw the V/V_{max} ratio. Within this framework, particular attention must be paid to the computation of individual V/V_a.

3. Theoretical background

3.1. Cosmology

The universe is described by a Friedman-Robertson-Walker model which is defined by three independent fundamental parameters (calculated at $z = 0$): the matter density Ω_m, which may include a non-baryonic component, the cosmological constant Ω_Λ, and the Hubble parameter H_0. The value of H_0 is very important for the creation of synthetic catalogues because it scales the distance and the absolute luminosity of the objects. Nevertheless, H_0 has no influence on individual $V/V_a's$, which are scale free. The other known cosmological parameters are related to these three parameters.

No arbitrary choice of a preferred cosmological model is made. General formulae for the distance and the volume are given in Caroll *et al.* (**?**). We define the conformal coordinate $\chi(z)$ as:

$$\chi(z) \;=\; 2\,|\Omega_K|^{1/2} \times \int_0^z \frac{dz'}{((1+z')^2(1+\Omega_m z') - z'(2+z')\Omega_\Lambda)^{1/2}} \quad ;$$

The volume out to redshift z is written:

$$V(z) = \left(\frac{c}{H_0}\right)^3 \frac{1}{2\Omega_K|\Omega_K|^{1/2}} \left[sinn(\chi(z)) - \chi(z)\right], \qquad (1)$$

where $\Omega_K = 1-\Omega_m-\Omega_\Lambda$ is the curvature, $sinn$ is sin if $\Omega_K < 0$ and $sinh$ if $\Omega_K > 0$. This equation is very useful for numerical computation because it does not require inverse trigonometric functions. Contrary to what happens in a closed universe, with the expressions given, e.g., in Caroll *et al.* (**?**), Eq.(1) is single valued and there is no discontinuity at the value $\chi = \pi$, as shown in Mathez *et al.* (**?**).

3.2. Evolution

The quasar population resides in an extremely young universe, and it has evolved up until the present epoch. It is likely that individual QSOs do not live for a long period of time, so we speak rather about the evolution in a statistical sense. In any case, assuming a PLE model for quasars amounts to assuming that the fraction of active quasars is constant with epoch, their luminosity decreasing with increasing time, and that they are in sufficient number so that we may apply this average evolutionary law to individual quasars in order to derive maximum redshifts. The absolute magnitude at redshift z is given by:

$$M(z) = M_0 - 2.5log_{10}(e(z)), \qquad (2)$$

where M_0 is the absolute magnitude at $z = 0$, and $e(z)$ is the evolutionary law:

$$e(z) \equiv (1+z)^{k_L} \qquad (3)$$

for a Power Law Luminosity Evolution (PWLE), and

$$e(z) \equiv exp\,(k_L t(z)/H_0) = exp\,(t(z)/\tau) \qquad (4)$$

for an Exponential Luminosity Evolution (LEXP); k_L is the evolutionary parameter, $t(z)$ the look-back time and τ the characteristic evolutionary time. Strictly speaking, as quoted by Bigot and Triay (**?**), this evolution law has only a statistical sense and does not apply to individual QSOs. However, to compute each V/V_a value, we fictitiously move each QSO toward high redshifts, and it is necessary to apply this evolution law to each QSO.

Assuming a power law spectrum $f_\nu = \nu^{-\alpha}$ with a spectral index $\alpha = 0.5$, the Mattig relation relates the observables (m, z) of a quasar to M_0, its absolute magnitude at $z = 0$:

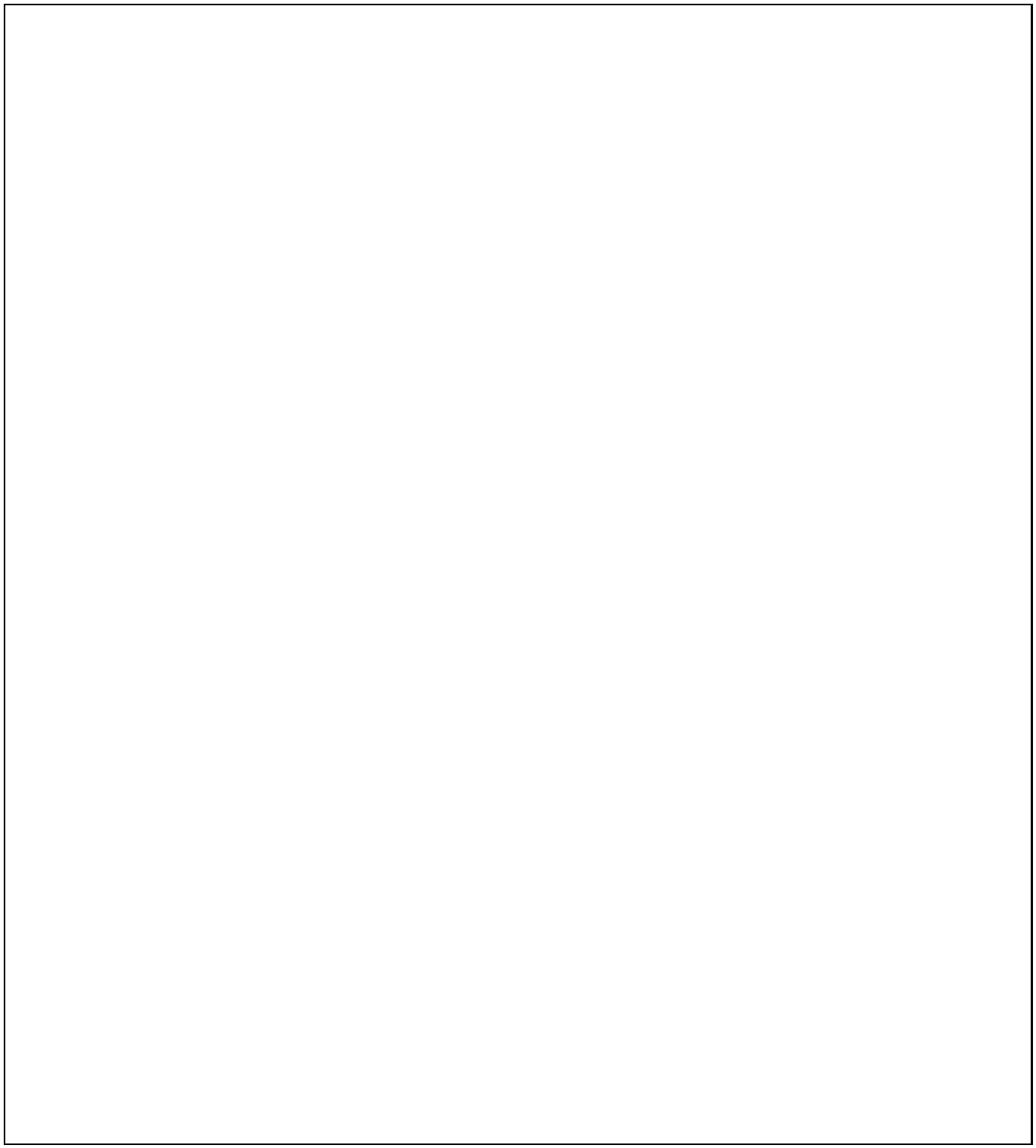

Fig. 1. Four possible *apparent magnitude − redshift* plots: monotonicaly increasing, one maximum, both one maximum and one minimum, and monotonicaly decreasing. The evolutionary tracks are drawn according to the cosmology and exponential luminosity evolution as described by the top labels. The $m = m(z)$ curves (solid lines) correspond to bins of constant width in absolute magnitude. The horizontal dashed line represents a constant limiting magnitude $B = 21$; the dashed $m(z)$ line corresponds to the faint separator $\mathcal{S}_2$ between magnitude-limited and redshift-limited quasars (see text). Depending on the parameters (cosmology and evolution), the same quasar may be either magnitude– or redshift–limited. In models where $m(z)$ shows a maximum (for example in Fig. 1b), for quasars lying between $\mathcal{S}$ and $B = 21$ there exists a redshift slice where $m(z)$ is above $B = 21$. The corresponding volume must be subtracted from the available volume $V_2 - V_1$. Quasars of the complete Boyle *et al.* (1990) sample are superimposed.

$$m_{M_0}(z) = M_0 - 5 + 2.5 log_{10}\left(\frac{d_L^2(z)K(z)}{e(z)}\right); \quad (5)$$

here $K(z) = (1+z)^{(\alpha-1)}$ is the K-correction.

The evolutionary tracks $m(z)$ on the Hubble diagram are shown in Fig. 1 for a given set of quasars in four different cosmologies and evolutionary histories. The curves appear to be quite different. In particular the quasars in Fig1.b,c,d become brighter and brighter as the redshift increases, because the evolution dominates the cosmological dimming at large z.

3.3. Distribution of the QSOs in the Hubble plane

Available complete QSO samples usually have a well defined limiting magnitude, towards faint magnitudes. Due to saturation effects (in the photometry or in the spectroscopy), a bright limiting magnitude may also apply.

All UVX QSOs are limited to redshifts $z \leq 2.2$, precisely because of their selection as objects with a UV excess, a standard way to detect quasars in optical astronomy. As the redshift decreases (below $z = 0.3$), there is another limitation because quasars become spatially resolved and can no longer be classified as stellar objects. These redshift limitations prevent the use of maximum (respectively minimum) redshifts outside the limiting redshifts of the sample. Assume that we have a QSO sample in the magnitude and redshift ranges $[m_1, m_2]$ and $[z_1, z_2]$, respectively. For UVX samples we would have z_1 =0.3 and z_2 =2.2.

We define $\Phi(M, z)$ as the LF at redshift z and at absolute magnitude M. However, for the case of PLE it can be written $\Phi(M(z))$; then all luminosity functions at different redshifts differ by an additive constant along the absolute magnitude axis. This allows us to work with the LF defined at a fixed epoch ($z = 0$) where $\Phi(M(z = 0)) = \phi(M_0)$, whatever the evolutionary law (**?**). The number of objects in the range of absolute luminosity $[M_0, M_0 + dM_0]$ and redshift $[z, z + dz]$ writes:

$$d^2N = \phi(M_0)\, dM_0\, H(m_2 - m)\, H(m - m_1) \times H(z_2 - z)\, H(z - z_1)\, \frac{dV}{dz},\ dz \quad ,$$

with the following notations:

- dV is the comoving volume element of the shell of redshift z to $z + dz$ in the solid angle ω of the survey;
- $\phi(M_0)$ is defined above;
- The four Heaviside functions are the selection function, ensuring that apparent magnitudes and redshifts remain inside 'box $\mathcal{B}$', or $[m_1, m_2] \otimes [z_1, z_2]$, the limitations due to the selection criteria.

We now define $\mathcal{D}$ as the domain in the Hubble plane where all quasars are redshift–limited.

Let z_{top} (respectively z_{bot}) be the redshift in the range $[z_1, z_2]$ at which the evolutionary track passes through the maximum (minimum) of the $m(z)$ curve. z_{top} (z_{bot}) is the same for all quasars, since their $m(z)$ curves are parallel, differing by an additive constant equal to the absolute magnitude. Consider a given absolute magnitude M_0, and let $m_{M_0,top}$ ($m_{M_0,bot}$) be the corresponding faintest (brightest) apparent magnitude in box $\mathcal{B}$:

$$m_{M_0,top} = \sup_{z\in[z_1,z_2]}[m_{M_0}(z)] = m_{M_0}(z_{top}); \quad m_{M_0,bot} = \inf_{z\in[z_1,z_2]}[m_{M_0}(z)] = m_{M_0}(z_{bot}). \quad (6)$$

$m_{M_0}(z)$ is the apparent magnitude corresponding to the absolute magnitude M_0 at redshift z. z_{top} is equal to z_2 in the case of little or no luminosity evolution. Consider the $m(z)$ curve corresponding to $m_{top} = m_2$: it is unique; let us call it the 'faint separator' $\mathcal{S}_2$. There is also a 'bright separator' – the unique curve $\mathcal{S}_1$ crossing $(z_{bot}, m_{bot} = m_1)$. $\mathcal{S}_2$ is drawn on Fig. 1. Domain $\mathcal{D}$ is simply the domain located *below* $\mathcal{S}_2$ and *above* $\mathcal{S}_1$. Let $M_0^{S_i}$ be the two absolute magnitudes corresponding to the curves $\mathcal{S}_i$, $(i = 1, 2)$. The domain $\mathcal{D}$ simply consists of that part of the Hubble plane brighter than $M_0^{S_2}$ and fainter than $M_0^{S_1}$. We call $\mathcal{D}^*$ the complement of $\mathcal{D}$ with respect to the box $\mathcal{B}$. We call $\mathcal{D}$ and $\mathcal{D}^*$ quasars the quasars located in each of these domains.

3.4. The V/V_{max} test

Since our method relies on V/V_a values, it is necessary to review the V/V_a computation, particulary in the case of strong evolution. Consider a quasar in the sample with (m, z) as its representative point in the Hubble diagram, and define the following quantities:

- M_0: the quasar absolute magnitude at epoch $z = 0$;
- $z_{max}(M_0, m_i)$ $(i = 1, 2)$: the redshift(s) where the quasar has an apparent magnitude m_i;
- $V_{max}(M_0, m_i)$: the corresponding comoving volume(s);
- V_a: the available volume;
- V_i $(i = 1, 2)$: the comoving volumes enclosed by the two limiting redshifts z_i.

The various possible shapes of the evolutionary track (Fig. 1) are crucial for understanding the V/V_a test. The quasar may leave the sample in one of two ways: either its magnitude leaves the range $[m_1, m_2]$, or its redshift leaves the range $[z_1, z_2]$. The available volume V_a does *not* reduce to $V_{max}(M_0, m_2)$: it is the total volume $V_2 - V_1$, minus $\sum V_{out}$, the sum of the volumes of all slices of the universe where the evolutionary track is outside box $\mathcal{B}$, so that it prevents the quasar from remaining in the sample.

Assuming that volumes are randomly distributed over the range $[V_1, V_2]$, the variable uniformly distributed over $[0, 1]$ is the ratio x defined below. The number of quasars in the redshift range $[z_1, z_2]$ is:

$$N = \int_{(M_0)_1}^{(M_0)_2} dM_0 \Phi(M_0) \int_{sup(z_1, z_{max}(M_0,m_1))}^{inf(z_2, z_{max}(M_0,m_2))} dz \frac{dV}{dz} = \int_{(M_0)_1}^{(M_0)_2} dM_0 \Phi(M_0) V_a(M_0), \quad (7)$$

where:

$$V_a(M_0) = inf(V_2, V_{max}(M_0, m_2)) - sup(V_1, V_{max}(M_0, m_1)) - \sum V_{out}. \quad (8)$$

Note that for $\mathcal{D}$ quasars $inf(z_2, z_{max}) = z_2$ and $sup(z_1, z_{min}) = z_1$ *simultaneously.*

It is straightforward to find the new variable x:

$$x = (V - V_{sup} - \sum V_{out})/(V_{inf} - V_{sup} - \sum V_{out}). \quad (9)$$

Indeed, one shows that the mean of the ratio x over the sample is 1/2:

$$< x > = \frac{1}{N}\int_{(M_0)_1}^{(M_0)_2} dM_0\Phi(M_0) \times \int_{V_{sup}}^{V_{inf}} dV \frac{(V - V_{sup} - \sum V_{out})}{(V_{inf} - V_{sup} - \sum V_{out})}$$

$$= 1/2, \qquad \forall\Phi, \forall(M_0)_1, \forall(M_0)_2;$$

moreover, since $dV = V_a(M_0)dx$, we have:

$$dN = \int_{(M_0)_1}^{(M_0)_2} dM_0\Phi(M_0)V_a(M_0)\ dx$$

$$= N\ dx,$$

which characterizes a PDF of x which is uniform over $[0, 1]$. For a redshift–limited sample over $[z_1, z_2]$, taking $V_{sup} = 0$ overestimates V/V_a and taking $V_{inf} = V_a$ underestimates V/V_a. In either case, $< x >$ cannot be equal to 1/2 *even in the correct cosmology and with the correct evolutionary law.*

Varying the shape of the evolutionary track changes the expression of the variable x. There may exist zero, one or several maxima of $m(z)$, or the quasar may become fainter than m_2 at low redshift; in fact there may be several roots of the equation $m(z) = m_2$. Fig. 1 shows various curves $m(z)$ for various cosmologies and evolutionary histories, in order to illustrate the existence of redshift ranges, lying inside the range $[z_1, z_2]$, but for which $m(z)$ is *not* in the range $[m_1, m_2]$. Such ranges must be excluded from the volume computation.

4. Luminosity Functions in real samples

The LF is not a direct observable – on the contrary it depends on the choice of the cosmological model and of the evolutionary law. For our purpose, it is necessary to be realistic in reproducing the data; in particular, the artificial catalogues must have the same LF as the real sample whatever the choice of their parent cosmological model.

As discussed in Kassiola and Mathez, (**?**), given the cosmology and the evolution, there are two ways to derive the LF from data: firstly one can construct the *Global Luminosity Function* (GLF), by shifting the absolute magnitudes of the whole sample to the present epoch $z = 0$, according to the evolution law, and secondly one can compute the *Restricted Luminosity Functions* (RLFs), i.e. the LFs in different redshift bins. A necessary condition for PLE to apply is that the LF in all redshift bins differ by a simple shift along the absolute magnitude axis. To do this, one has to compare the RLFs. Assuming that PLE is correct, the reason for choosing the GLF to construct the catalogues is to avoid the noise created by binning the data in redshift. In Section 4.3, we test the PLE hypothesis by comparing of the RLF and the GLF.

4.1. Real data: the Boyle et al. sample

The complete sample of UVX quasars of Boyle *et al.* (1990) is used. It contains 383 quasars, if we exclude the Narrow Emission Lines (NL) and the redshifts outside the range $[0.3, 2.2]$.

4.2. The Global Luminosity Function and its derivation

We now consider the computation of the GLF for any redshift– and magnitude limited–QSO sample. The sample is binned in absolute magnitude M_0 with bin width ΔM_0. Let N_i be the QSO number in the i^{th} absolute magnitude bin. The GLF in bin i is given by:

$$\phi^i_{obs}(M_0) = \sum_{\substack{j=1 \\ M_{0j}\in B_i}}^{N_i} \left(1/V^j_a\right), \tag{10}$$

$$B_i = \left[M_0 - \frac{\Delta M_0}{2}, M_0 + \frac{\Delta M_0}{2}\right], \tag{11}$$

with an error on ϕ:

$$\sigma^i_\phi = \left(\sum_j^{N_i} {V^j_a}^{-2}\right)^{1/2}. \tag{12}$$

For the case of the Boyle sample, none of the eight fields intersect; thus, the available volume follows directly from Eq. (8):

$$V_a = \sum_k^{N_{fields}} \omega_k \times \left[inf(V^k_{max}, V_2) - sup(V^k_{min}, V_1) - \sum V_{out}\right], \tag{13}$$

where ω_k is the solid angle of the k^{th} field.

The GLF looks similar for all of the cosmologies we tried. Special attention has been paid to some of the cosmological models (e.g. $\Omega = 0, \Lambda = 0$; $\Omega = 1, \Lambda = 0$; $\Omega = 0, \Lambda = 0.8$), by various authors which found that the LF is well fitted by either a single (**?**) or a double (**?**) power–law. We adopted the double power law–model in all cosmologies and for the two functional forms of evolution:

$$\phi_{model}(M_0) = \frac{\phi^\star}{10^{0.4(M_0 - M_\star)(\alpha+1)} + 10^{0.4(M_0 - M_\star)(\beta+1)}}; \tag{14}$$

$M_\star$ is the characteristic absolute magnitude of the two power–law distribution, i.e. the knee of the distribution. Absolute magnitudes for the quasars are computed according to Eq. (5). The evolution parameter k_L is computed by setting $< x >= 1/2$ for the whole sample. Such a procedure differs from current work (**?**; **?**), in which k_L is fitted like the other parameters. The free parameters $\phi^\star$, $M_\star$, α, and β are derived by a χ^2 minimization of the binned GLF:

$$\chi^2 = \sum_{i=1}^{N_{bin}} \left(\frac{\phi^i_{obs} - \phi_{model}}{\sigma^i_{\phi_{obs}}}\right)^2, \tag{15}$$

where N_{bin} is the number of absolute magnitude bins. An important difference with other LF computations is that we have only four free parameters.

Table 1 and Figs. 2 and 3 show a panel of GLFs computed for four different cosmologies, scaled to $H_0 = 50\ kms^{-1}Mpc^{-1}$. The general behaviour of the GLF is identical for the exponential and power–law evolutions. The GLF is enlarged and QSOs are brighter for a Λ–dominated universe. This is due to the

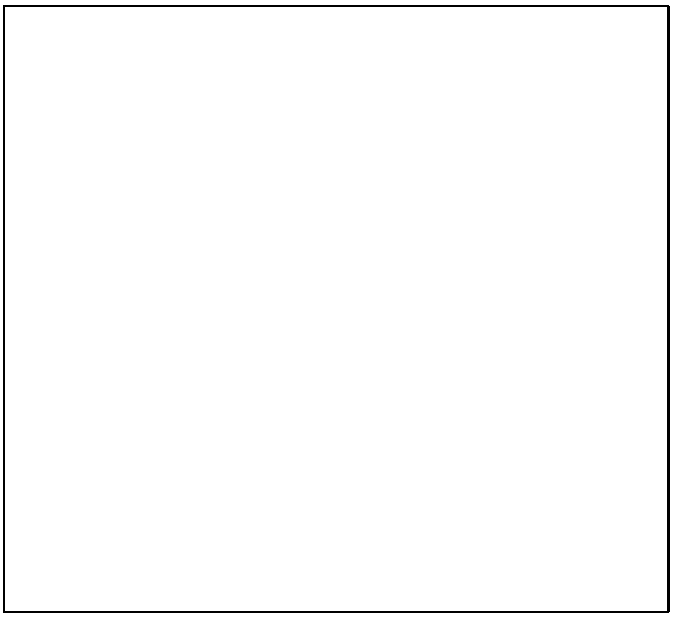

Fig. 2. Global Luminosity Functions in four cosmologies, for a power–law luminosity evolution. The models a, b, c, d of Table 1 progress from the larger to the thicker line.

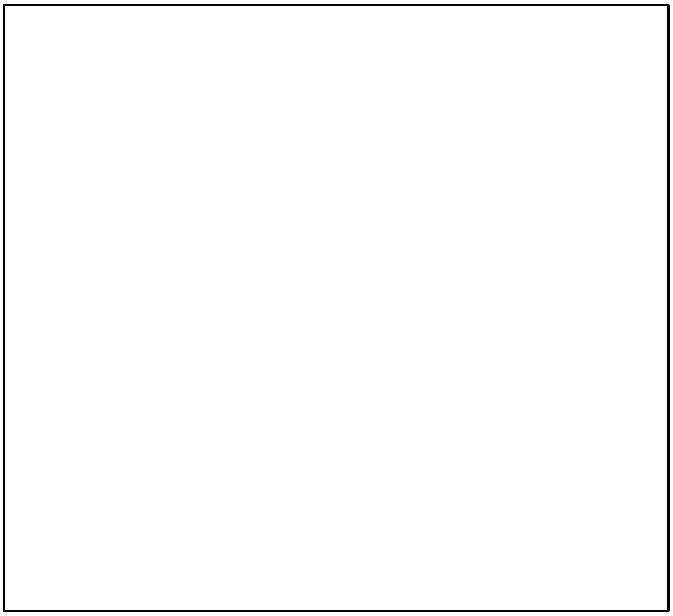

Fig. 3. Same as above, exponential luminosity evolution. The models e, f, g, h of Table 1 progress from the larger to the thicker line.

fact that, at fixed redshift, the distance in this type of model is greater than in other models, and therefore the absolute luminosities are larger. The effect is in the opposite sense for matter–dominated universes where the objects become fainter and the GLF narrower. The knee of the luminosity distribution evolves according to the preceding remarks. The faintest, shortest and densest GLF is obtained for $\Omega = 1$ and $\Lambda = 0$. The evolution becomes weaker in Λ-dominated universes but has a more standard value (k_L around 3–4 in PWLE models) if Ω is greater than 0.4, regardless of the value of Λ.

Despite our different LF computation method, we find results quite similar to those of Malhotra *et al.* (**?**) and Boyle *et al.* (**?**).

4.3. The Restricted Luminosity Functions

Restricted LFs (RLFs) have been computed from the Boyle sample in three different redshift bins ($[0.3, 1.0]$, $[1.0, 1.7]$, $[1.7, 2.2]$). We are interested in checking whether or not the PLE hypothesis is confirmed. If this is the case, any RLF may be deduced from the GLF by a simple shift along the absolute magnitude axis according to the evolution law (Eq. 2). Since we have computed the GLF in the last Section, we are able to compare our RLF to the GLF. This is done by a χ^2–procedure between the GLF and the three RLFs:

$$\chi^2 = \sum_{i=1}^{N_{bin}} \left(\frac{\phi_{GLF} - \phi^i_{RLF}}{\sigma^i_{\phi_{RLF}}} \right)^2 . \quad (16)$$

Here, ϕ^i_{RLF} and $\sigma^i_{\phi_{RLF}}$ refer to the RLF, computed from the data in the limited redshift bins, and ϕ_{GLF} is shifted to this redshift range.

The result is shown in Table 1 for four cosmologies and the two evolutionary models. The probabilities $P(> \chi^2)$ are high, and, except for one case (LEXP, $\Omega_{mat} = \Lambda = 1$), the test succeeds to better than the 15% confidence level. This result is in condradiction to those of a similar test done by Kassiola and Mathez (1991), which found strong discrepancies between the GLF and the RLF. However, they interpret these discrepancies as the lack of homogeneity of their composite catalogues. Since our results are consistent with PLE (favoured by Boyle *et al.*, 1987), we use this hypothesis to construct our synthetic catalogues.

5. Evolution characteristic time in various cosmologies

In the exponential model, the characteristic evolution time τ enters explicitely in Eq. (4), the expression for $e(z)$. This is not the case for the power law model – but a characteristic time may be defined as the look–back time to which all luminosities were higher by a factor e:

$$\tau = t\,(z_k = exp(1/k_L) - 1)\,. \quad (17)$$

Table 2 (3) gives the evolutionary parameters k_L for a grid of cosmological parameters in PWLE (LEXP). Table 4 (5) gives the corresponding PWLE (LEXP) characteristic times, computed according to Eqs. (17) and (4), respectively. These times are in units of the Hubble time H_0^{-1}. As is well known, the quasar evolution time is of the order of $H_0^{-1}/(7.7 \pm 3.5)$ for exponential evolution (**?**; **?**; **?**), strongly dependent on the cosmological model. For power–law evolution, the characteristic time is $H_0^{-1}/(3.7 \pm 0.6)$.

Tables 6 and 7 give the same characteristic times as Tables 4 and 5, but in units of the age of the universe in each cosmological model. With the exception of the $\Omega = 0$, $\Lambda = 1$ model, all ratios in Table 6 are close to 0.30 ± 0.02, implying that the characteristic evolution time is about equal to $1/(3.2 \pm 0.2)$ of the age of the universe, whatever the cosmological model, in PWLE models. In LEXP models, this ratio is $1/(6.7 \pm 0.9)$. The characteristic times in Tables 4 and 5, apparently quite dependent of the cosmology, are indeed surprinsingly constant when expressed in terms of the age of the universe.

6. An algorithm for producing quasar catalogues

6.1. The algorithm

Fixing the evolutionary law, the cosmology (including the choice of H_0) and the catalogue limits (i.e. m_1, m_2, z_1, z_2 which allow the box $\mathcal{B}$ and domains $\mathcal{D}$ and $\mathcal{D}^*$ to be defined), each QSO (m, z) is fully determined by the other pair of variables $(V/V_a, M_0)$. This is easy to understand from Fig. 1, where the Mattig functions appear. All of our previous discussion shows that under the PLE hypothesis (which was checked on the data), any sample is fully determined from its limiting magnitudes and redshifts, the GLF and a uniform distribution of the V/V_a. From the probability distribution function (PDF) of absolute magnitudes M_0, which is $\phi(M_0) \times V_a(M_0)$, and from the $V/V_a(M_0)$ ratios uniformly spread over $[0, 1]$, it is possible to draw Monte–Carlo catalogues.

The algorithm is shown in Fig. 4. Choosing the cosmology and a functional form for the evolution, the first part of the work is to compute the evolutionary parameter from the constraint $< V/V_a >= 0.5$, using the Boyle sample. At the same time, $V_a(M_0)$ is computed and used to obtain the GLF. In the second part, two series of random numbers, ϵ_1 and ϵ_2, are used to extract the V/V_a and the absolute magnitude M_0 of each object in the synthetic catalogue from the relations:

$$\epsilon_1 = V/V_a = \frac{V - V_{sup} - \sum V_{out}}{V_{inf} - V_{sup} - \sum V_{out}},$$
$$\epsilon_2 = \frac{\int_{-\infty}^{M_0} dM \phi(M) V_a(M)}{\int_{-\infty}^{+\infty} dM \phi(M) V_a(M)}.$$

Obtaining the redshifts and apparent magnitudes is straightforward from a simple inversion procedure. Synthetic catalogues have been produced in the past, where both a LF *plus* a redshift histogram were jointly fitted. As already explained, this method suffers from at least two problems: Essentially, the two distributions may be incompatible in different cosmologies. Our method has the advantage of avoiding these problems since we use only one distribution, the GLF, and the other distributions (redshift, magnitude) are derived only after the cosmology and the evolution have been fixed. The algorithm shown in Fig. 4 ensures the coherence of these distributions, moreover it takes the evolution into account very accurately. This is not obviously true in previous methods where it is not clear how the evolution intervenes. In fact, we used the Cosmological Principle to replace the redshift distribution of the standard method by demanding the uniformity of V/V_a. Moreover, the limiting magnitude and the redshift range for the synthetic sample may be different from their values in the input sample.

6.2. Redshift and Magnitude Histogrames

The input (**?**) and output (synthetic catalogue with the same observational biases) redshift histogrames are compared in Fig. 5 for models *b* and *f* of Table 1. Similarly, the histogrames of absolute magnitude are compared in Fig. 6. The fit is quite satisfactory for both models; this is true for all models we tried. It is possible to introduce various biases in the synthetic catalogues, depending on which sort of catalogue we want to simulate. For example, for UVX quasars it is well known that the color selection criteria introduce a deficiency of QSOs in the redshift range $[1.5, 1.8]$ (**?**). Moreover, QSOs are variable objects, which can be simulated by randomly selecting a magnitude variation in a pre–defined distribution function. Noise in the magnitude and redshift measurements may be simulated in the same way.

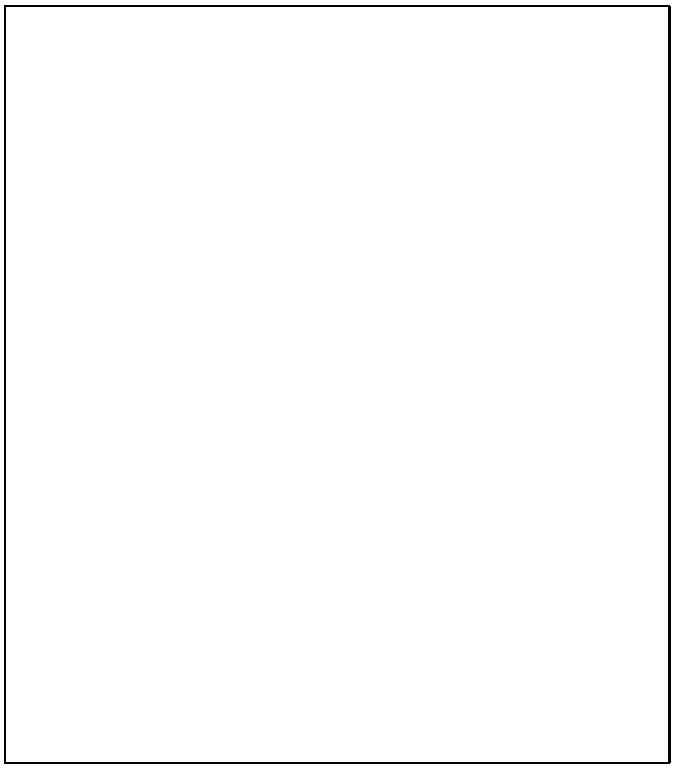

Fig. 4. Algorithm for the construction of synthetic catalogues

7. Conclusion

We have reviewed in detail the V/V_{max} computation in various cosmologies. The Mattig relation is used to understand how to compute the available volume V_a of a QSO, even in complicated cases. Both the Pure Luminosity Evolution (PLE) assumption and the Cosmological Principle allow the variables $(M_0, V/V_a)$ to be used instead of (m, z) to construct synthetic QSO samples in a coherent way. Some of the previous catalogue constructions were shown to suffer problems. The Global Luminosity Function used for this purpose is derived in a slightly different way from previous calculations since we fixed the evolution parameter by the condition $< V/V_a >= 1/2$. This significantly changes the value of this parameter, and hence of the GLF.

A surprising result is that the QSO characteristic evolution times are constant when expressed in terms of the age of the universe, regardless of the cosmology. The PLE hypothesis was checked on the data, which comfirms previous results (**?**). The advantage of such catalogues is that we tightly control all aspects of the sample: the parent cosmology, the strength and the functional form of the evolution, the luminosity function, the magnitude and redshift depths, and the effects of magnitude and redshift biases, all of which influence the results of the new cosmological test introduced in Paper I. In Paper I we apply the test to catalogues with different redshift limita-

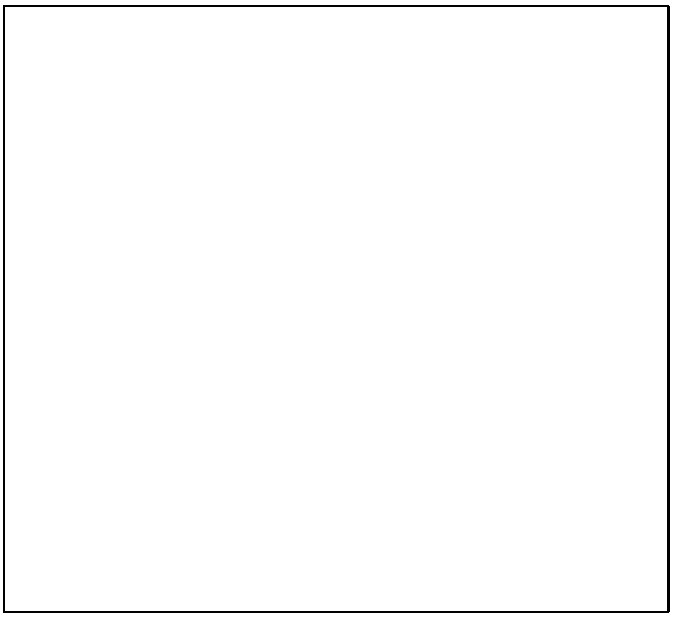

Fig. 5. Redshift Histogrames: (1): Boyle sample; (2): simulated catalogue, translated 15 upwards, model b; (3): idem, translated 35 upwards, model f

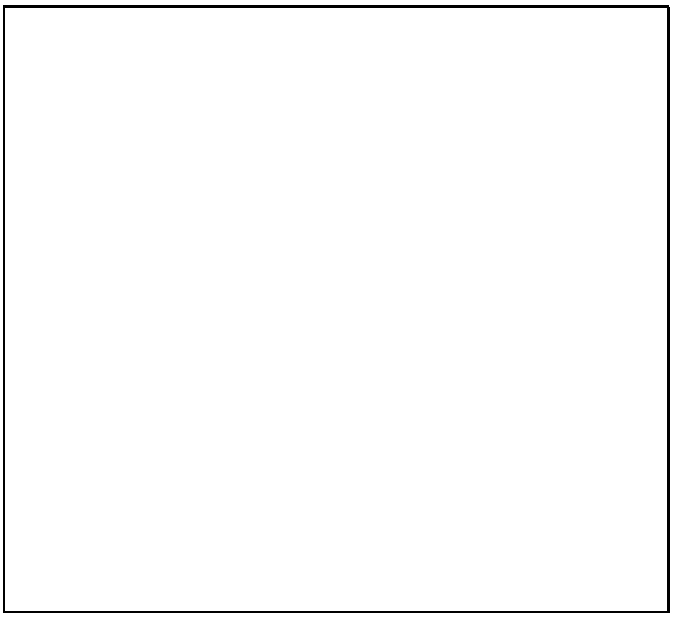

Fig. 6. Absolute Magnitude Histogrames: dashed curve: Boyle sample; full line: simulated catalogue, model b

tions, which leads us to propose a new observational strategy for the construction of future QSO samples. It is possible to test a catalogue with a wrong hypothesis, for example on the evolution, by assuming a power–law evolution and running the cosmological test with the exponential hypothesis. Moreover, our method is tractable with a Pure Density Evolution hypothesis, provided that density–weighted volume elements ρdV are substituted for all volume elements dV.

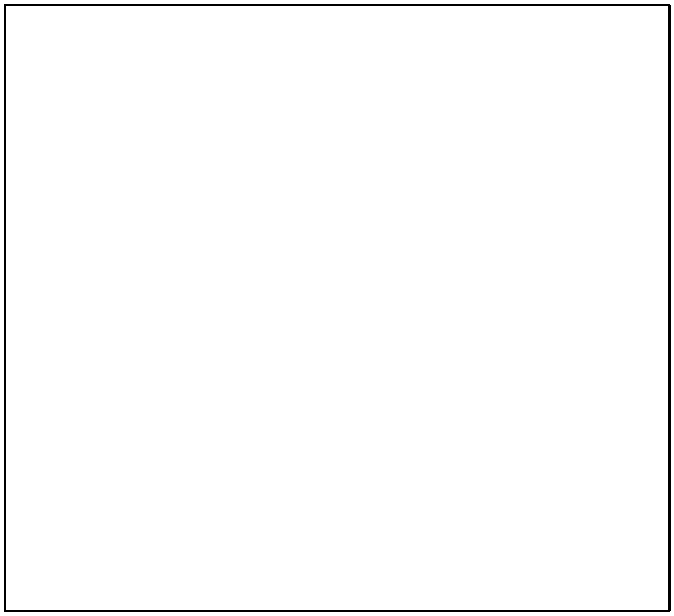

Fig. 7. Absolute Magnitude Histogrames: dashed curve: Boyle sample; full line: simulated catalogue, model f

Table 2. Power Law Luminosity Evolution (PWLE) parameter in different cosmologies. The model $\Omega = 0$, $\Lambda = 1$, which is marked with an asterisk, is close to a universe without a Big–Bang, and not very reliable.

Λ	Ω	0.0	0.2	0.4	0.6	0.8	1.0
0.0		2.94	3.16	3.28	3.44	3.50	3.60
0.2		2.88	3.13	3.28	3.47	3.50	3.63
0.4		2.78	3.10	3.28	3.47	3.53	3.66
0.6		2.66	3.06	3.28	3.47	3.60	3.69
0.8		2.47	3.00	3.31	3.47	3.63	3.75
1.0		1.91(*)	2.94	3.35	3.50	3.66	3.81

Table 3. Same as Table 2 for LEXP, Exponential Luminosity Evolution.

Λ	Ω	0.0	0.2	0.4	0.6	0.8	1.0
0.0		6.65	8.02	9.15	10.10	11.02	11.77
0.2		6.02	7.40	8.65	9.71	10.59	11.40
0.4		5.28	6.84	8.15	9.28	10.15	11.03
0.6		4.40	6.15	7.53	8.78	9.71	10.65
0.8		3.40	5.40	6.96	8.21	9.28	10.15
1.0		1.90(*)	4.59	6.28	7.65	8.78	9.71

Table 1. The LF (Eq. (10)) in various redshift ranges for four arbitrary cosmologies and two evolution laws. Since we are interested in input parameters to construct catalogues, confidence intervals are not needed. Only the best fit parameters are given. We choose $H_0 = 50 kms^{-1} Mpc^{-1}$.

	Ω	Λ	k_L	α	β	$M_\star$	$\phi^\star$ $10^{-6} Mpc^{-3}$	$P(>\chi^2)$ z_1 =0.3 z_2 =2.2	$P(>\chi^2)$ 0.3 1.0	$P(>\chi^2)$ 1.0 1.7	$P(>\chi^2)$ 1.7 2.2
PWLE											
a	0	0	2.94	-3.32	-1.38	-23.41	1.810^{-6}	0.97	0.20	0.78	0.80
b	1	0	3.60	-3.89	-1.30	-22.10	1.110^{-5}	0.99	0.99	0.69	0.92
c	0	1	1.91	-2.43	-1.23	-23.76	2.610^{-6}	0.89	0.15	0.88	0.58
d	1	1	3.81	-4.22	-1.37	-22.25	3.210^{-6}	0.99	0.92	0.66	0.81
LEXP											
e	0	0	6.65	-3.51	-1.49	-22.18	1.510^{-6}	0.99	0.58	0.78	0.40
f	1	0	11.8	-4.61	-1.55	-19.84	6.310^{-6}	0.97	0.88	0.57	0.24
g	0	1	1.90	-2.69	-1.49	-24.66	1.210^{-6}	0.76	0.16	0.23	0.58
h	1	1	9.71	-4.62	-1.60	-20.13	2.110^{-6}	0.99	0.64	0.57	0.01

Table 4. Evolution characteristic times: look–back time to which all luminosities were higher by a factor e, given the PWLE parameter in Table 2. Times are in units of H_0^{-1}, the mean is 0.27 and the dispersion is 0.04.

Λ Ω	0.0	0.2	0.4	0.6	0.8	1.0
0.0	.29	.27	.26	.24	.23	.23
0.2	.30	.28	.26	.24	.24	.23
0.4	.32	.29	.27	.25	.24	.23
0.6	.35	.30	.28	.25	.24	.24
0.8	.39	.31	.28	.26	.25	.23
1.0	.52(*)	.33	.29	.27	.25	.24

Table 5. Same as Table 4, but for LEXP. Mean characteristic time: 0.13; dispersion: 0.05.

Λ Ω	0.0	0.2	0.4	0.6	0.8	1.0
0.0	.15	.12	.11	.10	.09	.08
0.2	.17	.13	.12	.10	.09	.09
0.4	.19	.15	.12	.11	.10	.09
0.6	.23	.16	.13	.11	.10	.09
0.8	.29	.18	.14	.12	.11	.10
1.0	.53(*)	.22	.16	.13	.11	.10

Table 6. PWLE characteristic times (Table 4) in units of the age of the universe in the corresponding cosmology. Mean: 0.31; dispersion: 0.02. These ratios are far more independent of cosmology than the times in Table 4.

Λ Ω	0.0	0.2	0.4	0.6	0.8	1.0
0.0	.29	.32	.33	.33	.34	.34
0.2	.28	.31	.33	.32	.33	.34
0.4	.28	.31	.32	.32	.33	.33
0.6	.27	.30	.31	.31	.32	.32
0.8	.25	.29	.30	.30	.31	.31
1.0	.13(*)	.28	.29	.30	.30	.31

Acknowledgements We thank B. Fort, P.Y. Longarreti, G. Soucail, J.P. Picat, R. Pelló and J.F. Leborgne for support and discussions, and especially Jim Bartlett for a careful reading of the manuscript and enlighting suggestions. L.V.W. thanks the french MESR for grant 93135. This work was supported by grants from the french CNRS (GdR Cosmologie) and from the European Community (Human Capital and Mobility ERBCHRXCT920001).

Table 7. Same as Table 6, but for LEXP. Mean: 0.15; dispersion: 0.02. As for PWLE, the characteristic time depends far less on the age of the universe than on the Hubble time.

Λ	Ω	0.0	0.2	0.4	0.6	0.8	1.0
0.0		.15	.15	.14	.14	.13	.13
0.2		.16	.15	.14	.14	.13	.13
0.4		.16	.16	.15	.14	.13	.13
0.6		.17	.16	.15	.14	.13	.13
0.8		.19	.17	.15	.14	.13	.13
1.0		.13(*)	.18	.16	.14	.14	.13